Article

Chinese Science Bulletin

Materials Science

August 2011 Vol.56 No.23: 2475–2480
doi: 10.1007/s11434-010-4502-8

Layered Fe(III) doped TiO_2 thin-film electrodes for the photoelectrocatalytic oxidation of glucose and potassium hydrogen phthalate

YU Hua[1], WANG Jing[2,3], ZHANG ShanQing[1*], LI XinJun[2] & ZHAO HuiJun[1]

[1] *Environmental Futures Centre and Griffith School of Environment, Gold Coast Campus, Griffith University, QLD 4222, Australia;*
[2] *Guangzhou Institute of Energy Conversion, Chinese Academy of Sciences, Guangzhou 510640, China;*
[3] *Graduate University of the Chinese Academy of Sciences, Beijing 100049, China*

Received July 30, 2010; accepted November 5, 2010

Four types of TiO_2 thin-film electrodes were fabricated from TiO_2 and Fe(III) doped TiO_2 sols using a layer-by-layer dip-coating technique. Electrodes fabricated were TF (pure TiO_2 surface, Fe(III)-TiO_2 bottom layer), FT (Fe(III)-TiO_2 surface, pure TiO_2 bottom layer), TT (both layers pure TiO_2) and FF (both layers Fe(III)-TiO_2). The photoelectrochemical behavior of these electrodes was characterized using linear sweep voltammetry (LSV), electrochemical impedance spectroscopy (EIS) and steady-state photocurrent measurements in aqueous 0.1 mol L^{-1} $NaNO_3$ containing varying concentrations of glucose or potassium hydrogen phthalate (KHP). EIS and LSV results revealed that exciton separation efficiency followed the sequence of TF > TT > FT > FF. Under a constant potential of +0.3 V, steady-state photocurrent profiles were recorded with varying organic compound concentrations. The TF electrode possessed the greatest photocatalytic capacity for oxidizing glucose and KHP, and possessed a KHP anti-poisoning effect. Enhanced photoelectrochemical performance of the TF electrode was attributed to effective exciton separation because of the layered TF structure.

Fe(III)-doped TiO_2, charge separation efficiency, photoelectrocatalysis

Citation: Yu H, Wang J, Zhang S Q, et al. Layered Fe(III) doped TiO_2 thin-film electrodes for the photoelectrocatalytic oxidation of glucose and potassium hydrogen phthalate. Chinese Sci Bull, 2011, 56: 2475–2480, doi: 10.1007/s11434-010-4502-8

Photoelectrocatalysis offers a powerful method for the degradation and monitoring of organic compounds in wastewater [1–7]. Semiconductor photoanodes play an important role in these processes [7–9], and among them TiO_2 is widely used because of its excellent chemical and photochemical stability, and outstanding photoelectrochemical efficiency [10–13]. To further its use in applications, the photoelectrocatalytic efficiency of TiO_2 photoanodes needs to be improved, and many studies have focused on this goal. The most effective and practical approach to achieve this is to incorporate features to facilitate exciton separation, such as band-gap engineering. For example, mixed phase TiO_2 electrodes (i.e. anatase/rutile) may possess higher activity in the photoelectrocatalytic degradation of organic compounds than pure anatase electrodes because the electron-transfer pathway from anatase phase to rutile phase facilitates the separation of photoelectron and photohole, extending the lifetime of the photoelectron and photohole [14]. Other TiO_2 modifications such as Pt[15] and Ag[16] doping have also been shown to improve organic degradation efficiency in photoelectrocatalytic processes, perhaps due to the Pt or Ag nanoparticles acting as electron traps and preventing exciton recombination.

Metal ion doping [17,18] has also attracted significant attention for modifying TiO_2 thin-film electrodes because of its narrowing of the band gap, suppressing of exciton recombination, and improving of photoelectrocatalytic performance [19]. The doping effects of different metals on

*Corresponding author (email: s.zhang@griffith.edu.au)

TiO_2 film electrodes have been investigated extensively [20]. Our studies [16–21] indicated that both metal ion type and the doped composite hierarchical structure affected photoelectrocatalytic activity. The layered structure that favored the formation of the electron flow gradient was beneficial for the improvement of exciton separation and, therefore, photoelectrocatalytic activity [16–21].

In the current work, layered Fe(III) doped TiO_2 electrodes were fabricated from TiO_2 and Fe(III) doped sols using a layer-by-layer dip-coating technique. The effect of Fe(III) doping on TiO_2 electrode photoelectrocatalytic behavior was systematically investigated. The layered Fe(III) doped structure is expected to be beneficial for enhancing exciton separation and thus photoelectrocatalytic activity of TiO_2 thin-film photoanodes.

1 Experimental

1.1 Preparation of TiO_2 and Fe(III)-TiO_2 sols

The TiO_2 sol was prepared by the hydrolysis of tetrabutyl titanate as described in our previous report 16. Briefly, 68 mL of tetrabutyl titanate and 16.5 mL of diethanolamine were dissolved in 210 mL of absolute ethanol, with the mixture stirred vigorously for 1 h at room temperature (solution A). A mixture of 3.6 mL of H_2O and 100 mL of ethanol (solution B) was added dropwise to Solution A under continuous stirring. After stirring for 0.5 h, polyethylene glycol (PEG, M_w 2000 Daltons, 30% *w*/*w* of the solid TiO_2 sol) was added, and the resulting alkoxide solution was aged for 24 h at room temperature to subsequently form the TiO_2 sol.

The preparation of the Fe(III)-TiO_2 sol was the same as described above except that aqueous $Fe(NO_3)_3$ was added as solution B, rather than H_2O. The molar ratio of Fe/Ti was 0.5% for the Fe(III)-TiO_2 sol.

1.2 Preparation of thin- film electrodes

Thin-film electrodes were fabricated using a layer-by-layer dip-coating technique, from the TiO_2 and Fe(III)-TiO_2 sols. Fluorine-doped tin oxide (FTO) conductive glass was used as the substrate, and was pretreated sequentially with detergent, water and ethanol, and dried at 80°C. For the dip-coating process, FTO glass was dipped into the TiO_2 or Fe(III)-TiO_2 sol and withdrawn at a speed of 2 mm s^{-1}. Different types of TiO_2 thin-film electrodes were fabricated following the procedures in Table 1. Once the desired coating had been obtained, TiO_2 electrodes were dried in air at room temperature, and subsequently annealed in air at 500°C for 1 h. TiO_2 and Fe(III)-TiO_2 sol coatings were denoted as T and F, respectively, and four types of the TiO_2 film electrodes were obtained. These were TF (pure TiO_2 surface layer, Fe(III)-TiO_2 bottom layer), FT (Fe(III)-TiO_2 surface layer, pure TiO_2 bottom layer), TT (both layers pure TiO_2) and FF (both layers Fe(III)-TiO_2), as shown in Table 1.

Table 1 Coating sequences for the TiO_2 thin-film electrodes

Coating mode	Thin-film composition	
	Bottom	Surface
TT	10 coats of TiO_2	10 coats of TiO_2
TF	10 coats of Fe(III)-TiO_2	10 coats of TiO_2
FF	10 coats of Fe(III)-TiO_2	10 coats of Fe(III)-TiO_2
FT	10 coats of TiO_2	10 coats of Fe(III)-TiO_2

1.3 Photoelectrochemical measurements

Photoelectrochemical experiments were carried out at room temperature in a three-electrode cell with a quartz window for UV illumination, as shown in Figure 1. The TiO_2 film electrode, a saturated Ag/AgCl electrode and a platinum mesh were used as the working, reference and counter electrodes, respectively. Aqueous 0.1 M (1 M=1 mol L^{-1}) $NaNO_3$ was employed as the supporting electrolyte. The TiO_2 electrode was inserted into an electrode holder, and illumination was achieved with a 300W Xenon arc lamp (Trusttech, Beijing, China) with an UV band pass filter (UG-5, Schott). Electrochemical characterization by linear sweep voltammetry (LSV), electrochemical impedance spectroscopy (EIS) and steady-state photocurrent (i_{ph}) were measured by a CHI660A electrochemical workstation (CH Instruments, USA) under constant UV illumination (light intensity of 6.2 mW/cm^2 at 365 nm).

2 Results and discussion

2.1 Photoelectrochemical characterization

Electrochemistry is a powerful tool for studying charge transport and recombination processes at TiO_2/electrolyte interfaces [22]. In this work, TiO_2 film electrodes were initially characterized with EIS and LSV techniques. EIS Nyquist plots are commonly used to investigate charge transport resistance and exciton separation efficiency [23]. The size of the arc radius on the EIS Nyquist plot indicates the rate of photoelectrochemical reaction at the electrode [24],

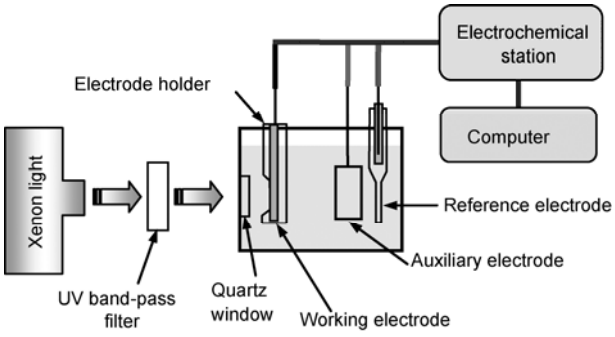

Figure 1 Schematic of the three electrode cell used for photoelectrochemical measurements.

and is a useful parameter for characterizing electron transport resistance [16]. Figure 2 shows impedance spectra of different TiO_2 film electrodes under UV illumination with light intensity of 6.2 mW cm^{-2} in aqueous 0.1 mol L^{-1} $NaNO_3$. Frequencies for EIS measurement were scanned from 10^5 to 0.1 Hz. The circular radii varied with doping, and were in the sequence TF < TT < FT < FF, as shown in Figure 2. This suggested that electron transport resistance of the electrodes was also in the sequence TF < TT < FT < FF.

The photoelectrochemical behavior of the TiO_2 electrodes was further characterized with LSV measurements in aqueous 0.1 mol/L $NaNO_3$ under the constant UV illumination [14]. The photocurrent originates from the photooxidation of water and organic compounds within the electrolyte, and photocurrent density corresponds to the amount of free carriers under the same potential bias, which is related to the amount of photo-generated holes within the TiO_2 electrode [16]. LSV curves of the TiO_2 electrodes are shown in Figure 3. Photocurrents of all samples increased with potential from –0.1 to 0.5V, and photocurrent values of the thin-film TiO_2 electrodes followed the sequence TF > TT > FT > FF. Under the same potential, stronger current indicates more electrons are collected from the photoelectrochemical reaction, and suggests better separation efficiency. The TF electrode showed the strongest photocurrent, and therefore exhibited the best exciton separation efficiency. The LSV result is coincident with that of the EIS measurement, because better exciton separation efficiency provides a higher free charge carrier concentration, leading to a lower electron transport resistance. Therefore the photocurrent sequence TF > TT > FT > FF is in agreement with the electron transport resistance order TF < TT < FT < FF.

An advantage of metal ion doping in TiO_2 is the temporary trapping of photo-generated charge carriers by the dopant, and the inhibition of their recombination during their migration from the materials core to surface [25]. For the electrodes fabricated in this study, Fe(III) ions present in

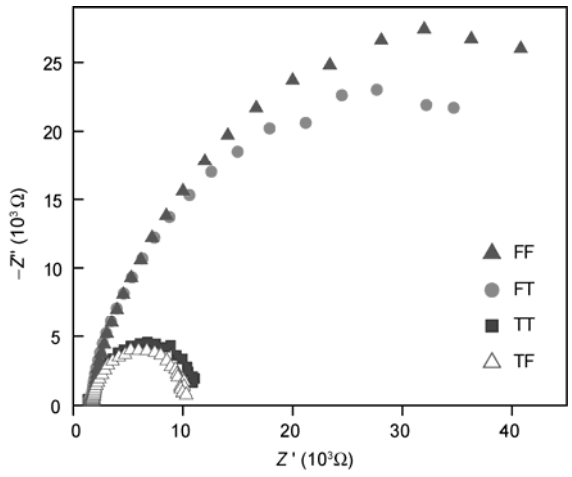

Figure 2 EIS Nyquist plots of the TiO_2 thin-film electrodes, under constant UV illumination.

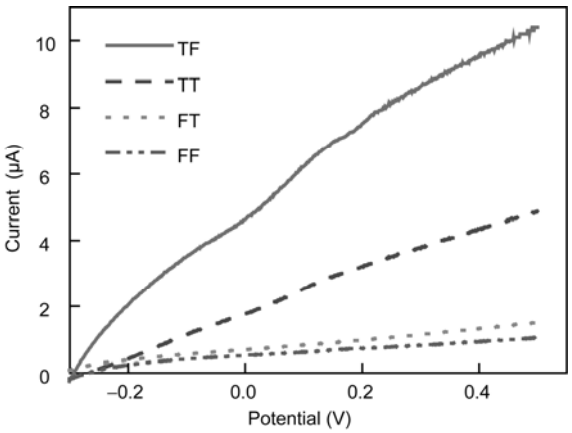

Figure 3 LSV plots for TiO_2 thin-film electrodes in aqueous 0.1 M $NaNO_3$ under constant UV illumination (scan rate was 5 mV s^{-1}).

the doped TiO_2 electrodes were expected to act as electron traps [26]. For the TF electrode, photo-generated electrons were attracted by the Fe(III) layer at the bottom of the electrode, and this attraction provided a further driving force for exciton separation at the electrode surface. Separation efficiency of the TF electrode was enhanced compared with that of the TT electrode, as evidenced by the lower electron transport resistance from EIS measurements and the higher photocurrent under the same potential from LSV measurements.

In contrast, the FT and FF electrodes had a much greater electron transport resistance and lower exciton separation efficiency than the TT electrode, for two reasons. First, part of the TiO_2 surface exposed to the UV light was covered by the Fe(III) species, so less charge carriers were generated under the same illumination conditions. Second, the additional attractive force on photo-generated electrons was towards the Fe(III) species at the FT electrodes top layer, and in opposing direction to the conductive substrate. In the photoelectrochemical process, electrons are removed from the conducting substrate at the bottom. Temporary trapping of electrons by Fe(III) on the surface hinders their subsequent removal. For the FF electrode, Fe(III) species were evenly distributed throughout, and such electron attraction processes affected the whole electrode. Because of these two effects, the FF and FT electrodes showed much larger electron transport resistance and lower photocurrent than the TT electrode.

2.2 Photoelectrochemical oxidation of organic compounds

TiO_2 based photoelectrocatalytic degradation is widely used in the treatment of wastewater, because it can oxidize a wide spectrum of organic compounds in aqueous solution 14. The general reaction for the complete mineralization of an organic compound, i.e. $C_yH_mO_jN_kX_q$, at the TiO_2 electrode surface can be represented by eq. (1) [13]:

Figure 4 shows a typical photocurrent response for a common TiO_2 electrode under a constant potential (+0.3 V *vs* AgCl/Ag) and constant UV illumination in aqueous solution. Upon illumination, a sharp current spike was observed, which was because of the oxidation of adsorpted water molecules and organic species. The current subsequently decreased gradually and obtained a steady-state. The overall steady-state photocurrent (i_{total}) is generally composed of two parts: one part (i_{net}) arises from oxidation of organic species (e.g. glucose or KHP), and the other (i_{water}) is due to water oxidation [14]. i_{net} can be calculated by subtracting i_{water} in the electrolyte without organic compounds, from i_{total} in electrolyte with organic compounds, as indicated in eq. (2). i_{net} represents the oxidation rate of the organic species[14], and is indicative of the organic compound concentration in solution [27].

$$i_{net} = i_{total} - i_{water}. \quad (2)$$

(i) Photoelectrochemical oxidation of glucose. Figure 5 shows i_{net} profiles of different TiO_2 film electrodes in aqueous 0.1 M $NaNO_3$ with increasing glucose concentration, under a potential bias of +0.3 V and UV illumination. TF electrodes showed the highest i_{net} for each concentration, and i_{net} values were found to follow the sequence TF > TT > FT > FF, consistent with the aforementioned LSV and EIS results. For all electrode types, i_{net} increased with glucose concentration and two distinct stages were observed. At low concentration, i_{net} increased linearly with glucose concentration. This was predominantly because of the mass transport limiting of organic compounds to the electrode surface. At higher concentrations, i_{net} deviated from linearity, and this was likely because of the saturated adsorption of glucose, with the photoelectrocatalytic reaction subsequently becoming the rate-determining step. The TF electrode possessed the highest i_{net} across both concentration ranges, which suggested that TF photoelectrocatalytic activity was greater than that of the other electrodes. The greatest photocatalytic activity was directly related to the largest number of photoholes on the TF surface, because of efficient exciton separation. The results also showed that i_{net} of FT and FF electrodes were smaller than that of the TT electrode. This suggested the FT and FF modification did not lead to positive improvement on the photocatalytic performance of the TiO_2 electrodes. This can also be rationalized with the aforementioned EIS and LSV measurements, because FT and FF modification did not lead to the net electron attraction force, only the loss of active sites due to Fe(III) coverage.

Overall, TF electrodes showed the highest photocurrent and photoelectrocatalytic oxidation efficiency, and glucose was easily oxidized because of the layered bottom-doping structure of the electrode.

(ii) Photoelectrochemical oxidation of KHP. Potassium hydrogen phthalate (KHP) is an aromatic organic compound, and because of the stability of the benzene ring, KHP is difficult to oxidize and can poison TiO_2 electrodes. Thus, it is frequently used as a standard degradation substrate for estimating photocatalytic efficiency of TiO_2 electrodes [28]. In this study, the photoelectrocatalytic degradation of KHP was carried out under the same experimental conditions as those for glucose above. Figure 6 shows i_{net} profiles for the oxidation of different KHP concentrations at the various electrodes. i_{net} values of all electrodes increased linearly with KHP concentrations in the low concentration range, similar to those observed for the oxidation of glucose because these i_{net} values were obtained under mass transport limitation. As shown in Figure 6, the linear ranges of KHP concentrations ended at 0.6, 0.5, 0.3 and 0.2 mM/L, for TF, TT, FT and FF electrodes, respectively. The TF electrode had the widest linear range, and it is well-established that electrodes with higher photoelectrocatalytic activity have a faster reaction rate and therefore a wider linear range [27]. The large amount of photo-holes provides a faster reaction rate and efficient oxidation of KHP. Thus, we concluded that TF had a higher photoelectrocatalytic oxidation capability

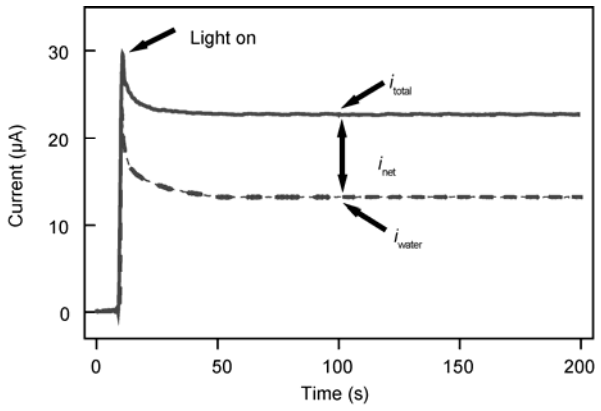

Figure 4 Typical photocurrent response of TiO_2 thin-film electrodes in aqueous 0.1 M $NaNO_3$ in the presence (solid line) and absence (dashed line) of organic compounds.

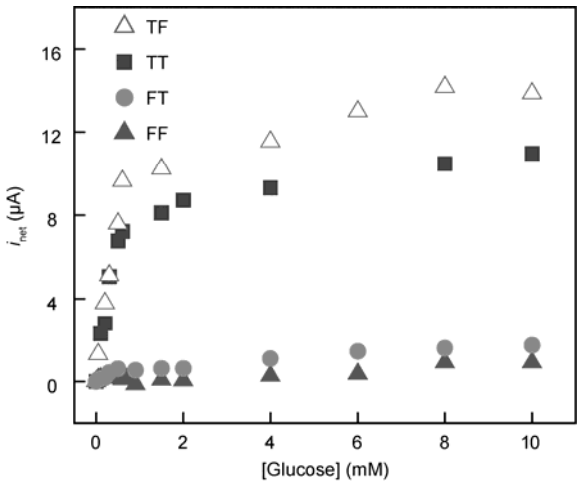

Figure 5 The relationship between glucose concentration and net photocurrent, i_{net}, for the four different electrode types.

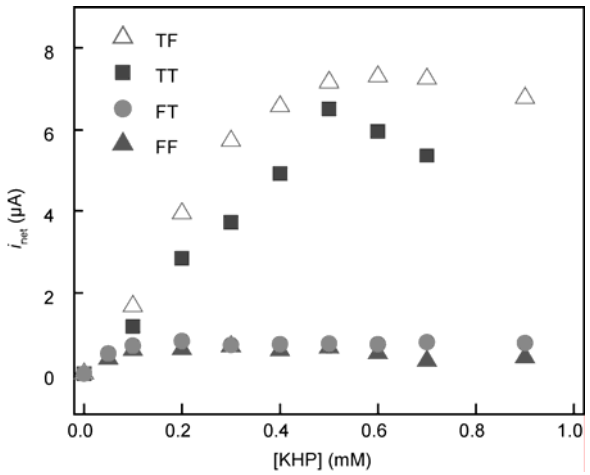

Figure 6 The relationship between KHP concentration and net photocurrent, i_{net}, for the four different electrode types.

than the other electrodes, attributed to the layered Fe(III) doped structure. This resulted in the best exciton separation efficiency among the four kinds of electrodes tested.

In contrast to the i_{net} profiles in Figure 5, i_{net} behaved differently after reaching its maximum in Figure 6. In Figure 6, with increasing KHP concentration, i_{net} for TT, FT and FF decreased, probably due to poisoning of the TiO_2 photocatalyst by the high KHP concentration [14–29]. An i_{net} decrease for TF was not observed, and i_{net} further increased with increasing KHP concentration. This suggested TF possessed an anti-poisoning effect, most likely because of the enhanced photocatalytic activity of the TF layered structure.

3 Conclusions

Layered Fe(III) doped TiO_2 electrodes were prepared by a dip-coating technique, and characterized using electrochemical methods. Electrode photocatalytic activity was evaluated by linear sweep voltammetry (LSV), and charge transport resistance was investigated by electrochemical impedance spectroscopy (EIS). EIS results demonstrated that TF thin-film electrodes possessed the greatest exciton separation efficiency. Greater separation efficiency results in more effective photoholes on the electrode surface for the photooxidation of water and organic compounds. This was confirmed by LSV measurements in aqueous solution with and without organic compounds. The highest photocurrent was obtained for the TF electrode, for both oxidizing water and the photoelectrocatalytic degradation of glucose and KHP. In addition, the TF electrode showed a promising KHP anti-poisoning effect.

The work was supported by the Australian Research Council (ARC), and the Knowledge Innovation Program of the Chinese Academy of Sciences (KGCX2-YW-343).

1 Zhao X, Qu J, Liu H. Photoelectrochemical degradation of anti-inflammatory pharmaceuticals at Bi_2MoO_6-boron-doped diamond hybrid electrode under visible light irradiation. Appl Catal B, 2009, 91: 539–545
2 Zhang X, Zhang Y, Quan X. Preparation of Ag doped $BiVO_4$ film and its enhanced photoelectrocatalytic (PEC) ability of phenol degradation under visible light. J Hazard Mater, 2009, 167: 911–914
3 Fraga L E, Anderson M A, Beatriz M L. Evaluation of the photoelectrocatalytic method for oxidizing chloride and simultaneous removal of microcystin toxins in surface waters. Electrochim Acta, 2009, 54: 2069–2076
4 Nissen S, Alexander B D, Dawood I. Remediation of a chlorinated aromatic hydrocarbon in water by photoelectrocatalysis. Environ Pollut (Oxford, U K), 2008, 157: 72–76
5 Selcuk H, Bekbolet M. Photocatalytic and photoelectrocatalytic humic acid removal and selectivity of TiO_2 coated photoanode. Chemosphere, 2008, 73: 854–858
6 Qu J, Zhao X. Design of BDD-TiO_2 hybrid electrode with P-N function for photoelectroatalytic degradation of organic contaminants. Environ Sci Technol, 2008, 42: 4934–4939
7 Yu S, Xi M, Han K. Preparation and photoelectrocatalytic properties of polyaniline/layered manganese oxide self-assembled film. Thin Solid Films, 2010, 519: 357–361
8 Esquivel K, Arriaga L G, Rodriguez F J. Development of a TiO_2 modified optical fiber electrode and its incorporation into a photoelectrochemical reactor for wastewater treatment. Water Res, 2009, 43: 3593–3603
9 Zhang H, Chen G, Bahnemann D W. Photoelectrocatalytic materials for environmental applications. J Mater Chem, 2009, 19: 5089– 5121
10 Palmisano G, Loddo V, El Nazer H. Graphite-supported TiO_2 for 4-nitrophenol degradation in a photoelectrocatalytic reactor. Chem Eng J, 2009, 155: 339–346
11 Osugi M E, Umbuzeiro G A, De Castro F J V. Photoelectrocatalytic oxidation of remazol turquoise blue and toxicological assessment of its oxidation products. J Hazard Mater, 2006, 137: 871–877
12 Egerton T A, Janus M, Morawski A W. New TiO_2/C sol-gel electrodes for photoelectrocatalytic degradation of sodium oxalate. Chemosphere, 2006, 63: 1203–1208
13 He C, Shu D, Xiong Y. Comparison of catalytic activity of two platinised TiO_2 films towards the oxidation of organic pollutants. Chemosphere, 2006, 63: 183–191
14 Jiang D, Zhang S, Zhao H. Photocatalytic degradation characteristics of different organic compounds at TiO_2 nanoporous film electrodes with mixed anatase/rutile phases. Environ Sci Technol, 2007, 41: 303–308
15 Ohtani B, Iwai K, Nishimoto S. Role of platinum deposits on titanium(IV) oxide particles: Structural and kinetic analyses of photocatalytic reaction in aqueous alcohol and amino acid solutions. J Phys Chem B, 1997, 101: 3349–3359
16 Zheng J, Yu H, Li X. Enhanced photocatalytic activity of TiO_2 nano-structured thin film with a silver hierarchical configuration. Appl Surf Sci, 2008, 254: 1630–1635
17 Peng B, Meng X, Tang F. General synthesis and optical properties of monodisperse multifunctional metal-ion-doped TiO_2 hollow particles. J Phys Chem C, 2009, 113: 20240–20245
18 Gomathi D L, Narasimha M B. Structural characterization of Th-doped TiO_2 photocatalyst and its extension of response to solar light for photocatalytic oxidation of oryzalin pesticide: A comparative study. Cent Eu J Chem, 2009, 7: 118–129
19 Yang Y, Li X J, Chen J T. Effect of doping mode on the photocatalytic activities of Mo/TiO_2. J Photochem Photobio A, 2004, 163: 517–522
20 Dorjpalam E, Takahashi M, Yoko T. Cr^{3+}-TiO_2 thin-film electrodes. Effects of the homogeneous and sectional doping. J Electrochem Soc, 2006, 153: 534–538
21 Yu H, Li X J, Zheng S J. Photocatalytic activity of TiO_2 thin film non-uniformly doped by Ni. Mater Chem Phys, 2006, 97: 59–63
22 Bao S J, Li C M, Zang J F. New nanostructured TiO_2 for direct electrochemistry and glucose sensor applications. Adv Funct Mater,

2008, 18: 591–599
23 Spagnol V, Sutter E, Debiemme-Chouvy C. EIS study of photo-induced modifications of nano-columnar TiO_2 films. Electrochim Acta, 2009, 54: 1228–1232
24 Liu H, Cheng S, Wu M. Photoelectrocatalytic degradation of sulfosalicylic acid and its electrochemical impedance spectroscopy investigation. J Phys Chem A, 2000, 104: 7016–7020
25 Choi W, Termin A, Hoffmann M R. The role of metal ion dopants in quantum-sized TiO_2: Correlation between photoreactivity and charge carrier recombination dynamics. J Phys Chem, 1994, 98: 13669–13679
26 Zhu J, Zheng W, He B. Characterization of Fe-TiO_2 photocatalysts synthesized by hydrothermal method and their photocatalytic reactivity for photodegradation of XRG dye diluted in water. J Mol Catal A Chem, 2004, 216: 35–43
27 Zhang S, Li L, Zhao H. A portable photoelectrochemical probe for rapid determination of chemical oxygen demand in wastewaters. Environ Sci Technol, 2009, 43: 7810–7815
28 Alhakimi G, Studnicki L H, Al-Ghazali M. Photocatalytic destruction of potassium hydrogen phthalate using TiO_2 and sunlight: Application for the treatment of industrial wastewater. J Photochem Photobiol A, 2003, 154: 219–228
29 Zhang J, Zhou B, Zheng Q. Photoelectrocatalytic COD determination method using highly ordered TiO_2 nanotube array. Water Res, 2009, 43: 1986–1992